JOURNAL OF MATERIALS SCIENCE 30 (1995) 2866–2872

A study of ionic defects in modified lead titanate ceramics

J. DE FRUTOS
ETSIT Avenida Complutense s/n, 28040-Madrid (Spain)
M. L. CALZADA*
Instituto Ciencia de Materiales de Madrid (CSIC), C/Serrano 144, 28006-Madrid (Spain)
E. MENÉNDEZ
ICCET/CSIC C/Serrano Galvache s/n, 28033-Madrid (Spain)

$Pb_{1-x}Ca_x[(Co_{0.5}W_{0.5})_{0.05}Ti_{0.95}]O_3$ ceramics with $x = 0.24$, 0.30 and 0.35, are prepared by a solid state reaction of oxides. Deviations from nominal chemical compositions and formation of segregated phases different from modified lead titanate perovskites, are studied. Pyro- and non-pyroelectric currents excited in the material by a thermal wave are investigated and related to mobility of electrical charges in the materials.

1. Introduction

Chemically modified lead titanate materials have aroused interest due to their highly anisotropic electromechanical properties [1]. $Pb_{1-x}Ca_xTi_{0.96}(Co_{1/2}W_{1/2})_{0.04}O_3$ ceramics with x between 0.12 and 0.24 have been prepared by Yamashita *et al.* [2]. The increase in modifiers results in a reduced tetragonality, c/a, and Curie temperature, T_c, when compared to pure $PbTiO_3$ perovskite.

Mechanical and electrical properties of the former ceramics are affected by the amounts of modifier cations and by the processing conditions. Besides, in lead titanate based compositions, limitations in properties often occur due to the presence of defects and residual intergranular phases that result from processing conditions [3]. Perovskite lattices are usually Pb-deficient because of the high volatility of PbO at the annealing temperatures [4]. This deficiency in lead brings about ionic defects in the crystal structure which can migrate under the high electric fields required for poling modified lead titanate ceramics. Therefore, defects play an important role in electromechanical properties of these materials [5].

It is the aim of this work to study the formation of ionic defects in modified lead titanate ceramics prepared by solid state reaction of oxides. The influence of these charged species in the electrical response of these materials is shown.

2. Experimental procedure

2.1. Chemical Processing

Modified lead titanate ceramics were prepared according to the following nominal chemical compositions [2]

$$Pb_{0.76}Ca_{0.24}[(Co_{0.5}W_{0.5})_{0.05}Ti_{0.95}]O_3 + 1\%\ MnO \quad PTC\text{-}24$$

$$Pb_{0.70}Ca_{0.30}[(Co_{0.5}W_{0.5})_{0.05}Ti_{0.95}]O_3 + 1\%\ MnO \quad PTC\text{-}30$$

$$Pb_{0.65}Ca_{0.35}[(Co_{0.5}W_{0.5})_{0.05}Ti_{0.95}]O_3 + 1\%\ MnO \quad PTC\text{-}35$$

To obtain these materials, stoichiometric mixtures of TiO_2, PbO, $CaCO_3$, $CoCO_3$ and WO_3 were prepared (Fig. 1). $Mn(NO_3)_2$ and HNO_3 with a $Mn(NO_3)_2/HNO_3 = 1$ molar ratio and 1% by weight of MnO with respect to the final calcium modified lead titanate perovskites, were added to the former mixtures. Manganese oxide was used to increase the electrical resistivity of the sintered ceramics [6]. To enhance reactivity of these systems, HNO_3 was added to the mixtures in an appropriate stage of the processing [7].

Synthesis of powders was made in air atmosphere at 850 °C for 3 h. A set of discs of each type of powder was isostatically pressed at 2000 kg cm^{-3}, and then sintered at 1050 °C for 3 h, with a constant heating rate of 3 °C min^{-1}.

2.2. Ceramic characterization

Bulk densities of each set of discs (PTC-24, PTC-30 and PTC-35) were calculated by Archimedes method. The average bulk densities, d_b, obtained from the former measurements are shown in Table I.

* Author to whom all correspondence should be addressed.

0022–2461

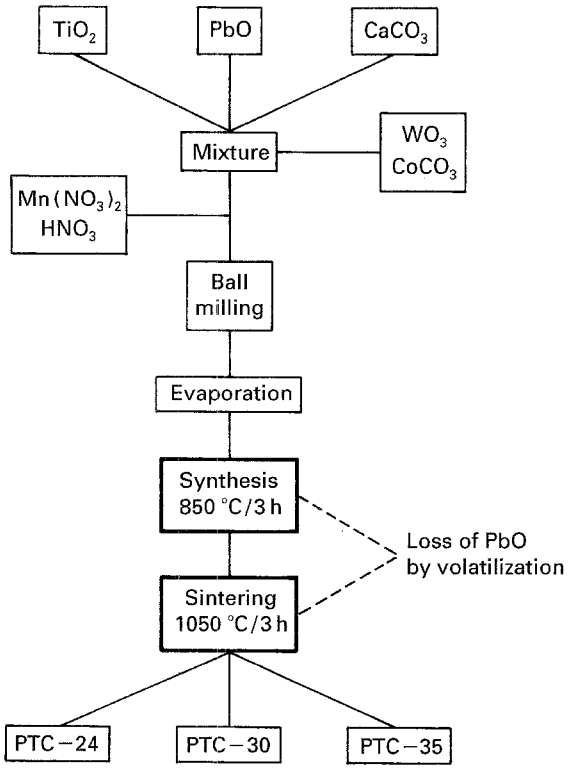

Figure 1 Processing for the preparation of modified lead titanate ceramics.

TABLE I Ceramic parameters of modified lead titanate ceramics

Material	d_b(g cm^{-3})	d_c(g cm^{-3})	F	c/a	V(Å^3)
PTC-24	6.77	6.94	0.97	1.039	63.761
PTC-30	6.46	6.89	0.94	1.030	61.761
PTC-35	6.33	6.86	0.92	1.019	60.091

d_b = bulk density, d_c = crystal density, F = packing factor, c/a = tetragonal distortion, V = unit cell volume.

X-ray diffraction analysis (XRD) was used to identify crystal phases present in the materials. Modified lead titanate perovskite was the only crystal phase observed in the X-ray diffraction patterns of Fig. 2. Tetragonality of perovskite, c/a, and volume of unit cell, a^2c, decreased with the increase of calcium content in the crystal (Table I).

Unit cell densities, d_c, were calculated from compositions and unit cell volumes. Comparison between unit cell and bulk densities allowed to obtain the packing factors, F, of the ceramics that also decreased with calcium content (Table I).

Microstructures of PTC-24, PTC-30 and PTC-35 sintered ceramics were studied using scanning electron microscopy (SEM) and energy dispersion X-ray analysis (EDXA).

2.3. Electrical measurements

PTC-24, PTC-30 and PTC-35 sintered samples were cut into discs of 0.8 mm thickness and 12 mm diameter, and electroded with vacuum evaporated silver.

These samples were poled with different electric fields at 120 °C. The active pole of the electric source was the negative one. It was connected to one of the sample faces denoted as face (−). The positive

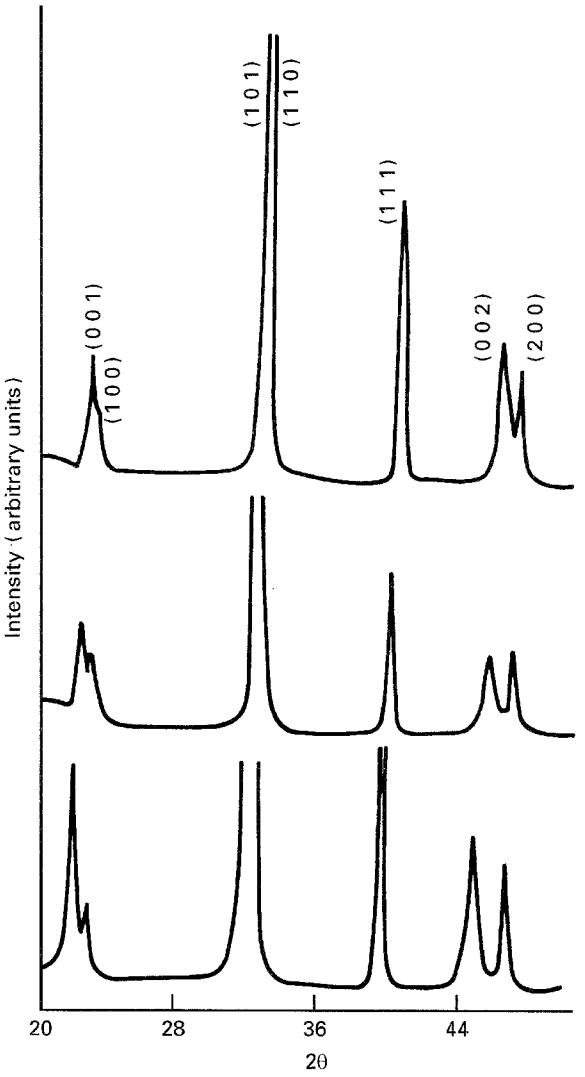

Figure 2 X-ray diffraction patterns.

pole was the earth of the electric source and it was connected to the other face of the studied sample, face (+). Piezoelectric charge coefficients, d_{33}, were measured using a Berlincourt–Piezo d_{33}-meter, at 100 Hz.

To study mobility of electric charge carriers in these ceramics, their intensity responses produced by a thermal wave are studied using a method developed by Frutos and Jiménez [8]. This method uses the equipment shown in Fig. 3 for generation and measurement of thermal currents in the former materials.

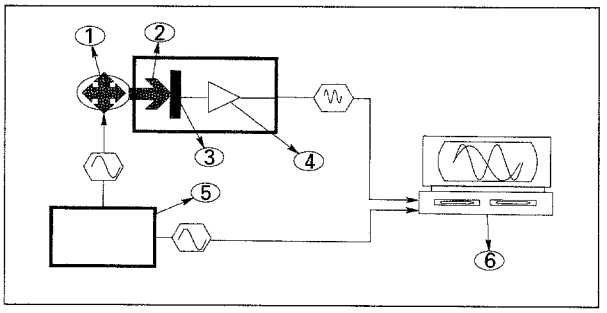

Figure 3 Equipment for generation and measurements of thermocurrents in materials. 1 Incandescence lamp (6 V, 0.01 A); 2 Fused quartz rod (l = 8 cm, ϕ = 0.5 cm) leads the lamp light to the sample: 3 Isolated and shielded sampleholder (turns 180° to face each sample face alternatively to the height of the incandescence lamp); 4 Low noise current amplifier (G = 10°); 5 Function generator HP3325B (supplies a sinusoidal voltage at frequencies between 10^{-6} and 10^6 Hz); 6 Data recorder and analyser.

To the lamp (1) is applied a current $I = I_o \sin(w_o t)$ (5) which produces an increase in the temperature of the sample (3) proportional to the thermal wave

$$T_f = T_{fo}\sin^2(w_o t) = [T_{fo}/2][1 - \cos(2w_o t)] \quad (1)$$

where T_{fo} = thermal wave amplitude, w_o = frequency and t = time.

Considering the heating cycle as positive and the cooling cycle as negative, a sinusoidal thermal wave is obtained

$$T_s = T_{so}\cos(2w_o t) \quad T_{so} = T_{fo}/2 \quad (2)$$

Under these conditions, a total alternate current of the sample, i, is measured in (6)

$$\begin{aligned} i_t &= RT + pA(dT/dt) = i_s + i_p \\ &= -i_{so}\cos(2w_o t) + i_{po}\sin(2w_o t) \\ &= i_{to}\sin(w_1 t + \theta) \end{aligned} \quad (3)$$

where $i_{so} = RT_{so}$, $i_{po} = pA2w_o$ (p = pyroelectric coefficient, A = sample area and $w_1 = 2w_o$). From the former equation, the phase component of the current $i_{so} = i_{to}\sin\theta$, nonpyroelectric intensity, and the $\Pi/2$ phase displacement component of the current, pyroelectric intensity, $i_{po} = i_{to}\cos\theta$ are obtained.

According to other authors [9, 10], non-pyroelectric currents are related to spatial charge distribution in the material. To get these distributions, currents were measured in the three types of ceramic samples [PTC-24, PTC-30 and PTC-35] on both faces [(−) and (+)] and with different electric poling fields, E_p. Pyroelectric and non-pyroelectric components of the currents were obtained.

3. Results and discussion

After synthesis, moulding and sintering of the three types of powders, modified lead titanate ceramics are obtained. Diffraction patterns of the ceramics (PTC-24, PTC-30 and PTC-35) are shown in Fig. 2. Tetragonal distortions and volume of unit cells calculated from the former patterns are close to the theoretical crystal parameters of these lead titanate based materials [2]. However, microanalysis by EDXA on the sintered ceramics show divergences with their nominal chemical compositions and segregation of phases [11].

Figs 4a, 5a and 6a are the calculated nominal compositions of PTC-24, PTC-30 and PTC-35. These compositions are not correspondent with results measured on the ceramics by EDXA (Figs 4b, 5b and 6b). They indicate a lack of lead and excesses of titanium, calcium and tungsten in sintered materials. Besides, enrichments in titanium, manganese and cobalt (Figs 4c, 5c and 6c) are measured in some areas of the ceramic microstructures (Fig. 7). It indicates formation of secondary phases clearly different in chemical composition from the general grain microstructure [12].

Lead defect in these ceramics is due to volatilization of PbO during synthesis and sintering [13]. Loss of PbO produces an imbalance in chemical composition and, as a consequence, the occurrence of free oxides of

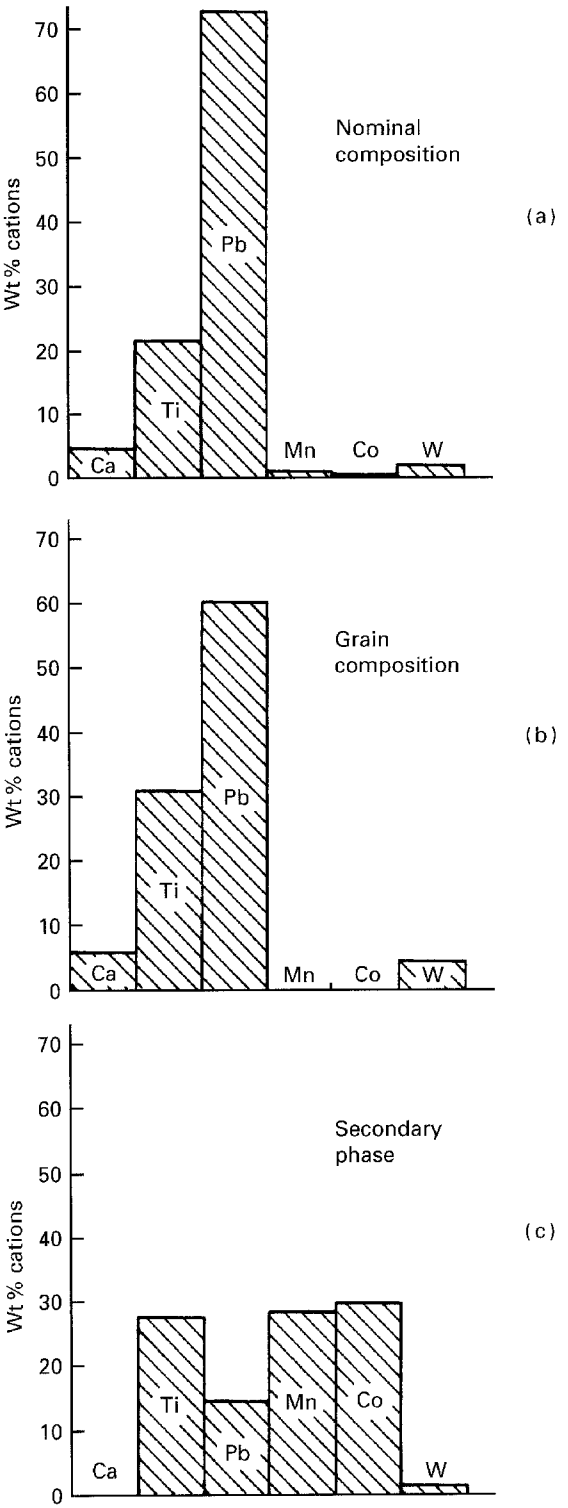

Figure 4 Chemical compositions of PTC-24 ceramics. (a) Nominal chemical composition; (b) chemical composition of the material measured by EDXA; (c) chemical composition of the segregated phases measured by EDXA.

titanium, calcium, cobalt and tungsten. Thus, crystals became lead and oxygen deficient according to the following solid state reaction [14]

$$\begin{aligned} &(1 - x - y)\mathrm{PbO} + (x + y')\mathrm{CaO} + (1 + y') \\ &\times[0.025(\mathrm{CoO} + \mathrm{WO_3}) + 0.95\mathrm{TiO_2}] + \mathrm{MnO} \\ &\rightarrow \mathrm{Pb_{1-x-y}Ca_x[(Co_{0.5}W_{0.5})_{0.05}Ti_{0.95}]O_{3-y}[I]} \\ &+ y'\mathrm{CaO} + y'[0.025\mathrm{CoO} + 0.025\mathrm{WO_3} \\ &+ 0.95\mathrm{TiO_2}] + \mathrm{MnO} \end{aligned} \quad (4)$$

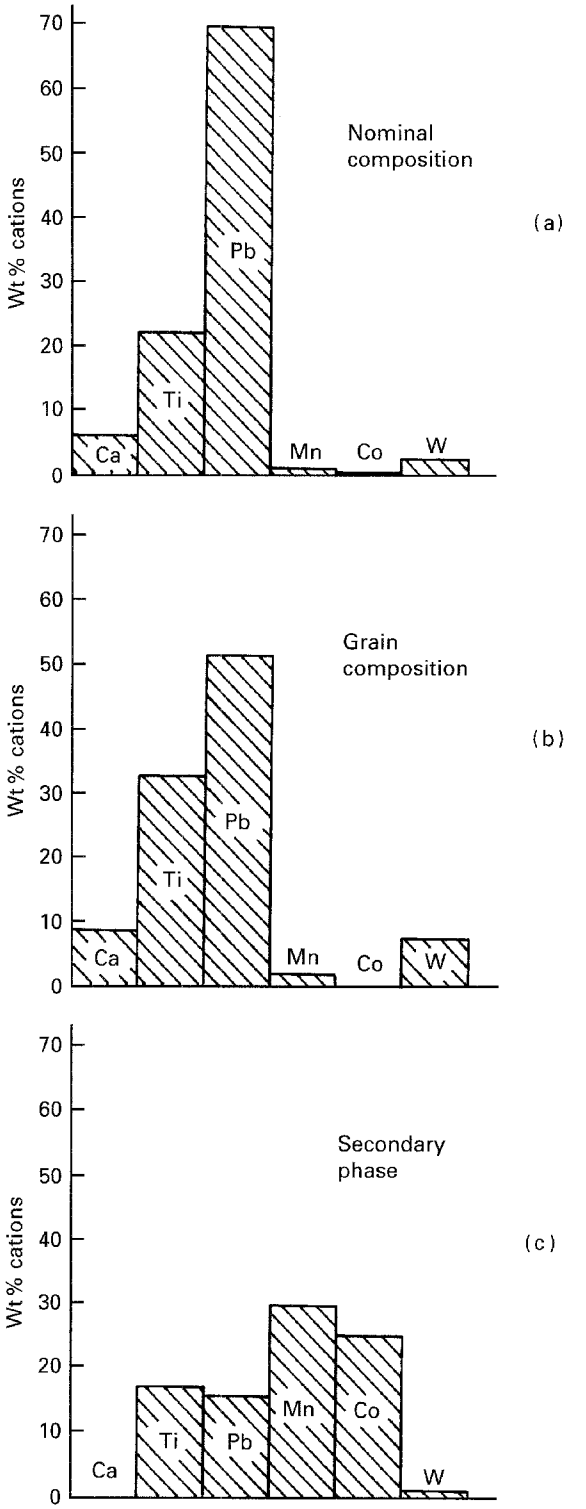

Figure 5 Chemical compositions of PTC-30 ceramics. (a) Nominal chemical composition; (b) chemical composition of the material measured by EDXA; (c) chemical composition of the segregated phases measured by EDXA.

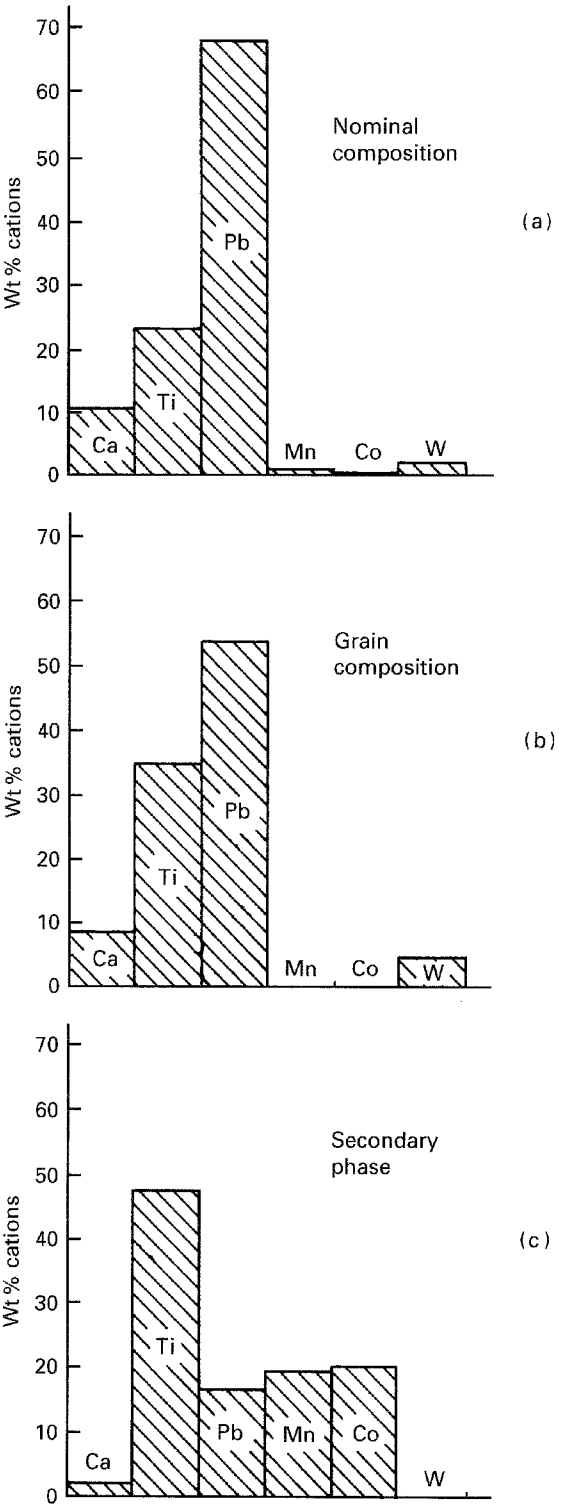

Figure 6 Chemical compositions of PTC-35 ceramics. (a) Nominal chemical composition; (b) chemical composition of the material measured by EDXA; (c) chemical composition of the segregated phases measured by EDXA.

where x is the quantity of calcium that substitutes lead, y is the unknown quantity of lead oxide lost by volatilization and y' is the excess of the other oxides that participate in the reaction.

The description as $Pb_{1-x-y}\square_{Pby}Ca_x[(Co_{0.5}W_{0.5})_{0.05}Ti_{0.95}]O_{3-x}\square_{Oy}$ instead of [I], enables the materials containing defects [15].

It has been shown before for pure lead titanate [14] that reaction between equimolar mixtures of oxides leads to Pb and O deficiencies in perovskite structure. These deficiencies are present as vacancies because of the close-packed arrangement of Pb and O in the crystal.

Lattice vacancies are also created thermally by substitution of ions with incorrect valencies [16]. Co^{2+} and W^{6+} ions which substitute Ti^{4+}, create oxygen vacancies in the modified lead titanate lattice [17]. For metals such as Mn, less is known about the way in which this element is incorporated, because of the different valence states that it can use [18]. Besides, it

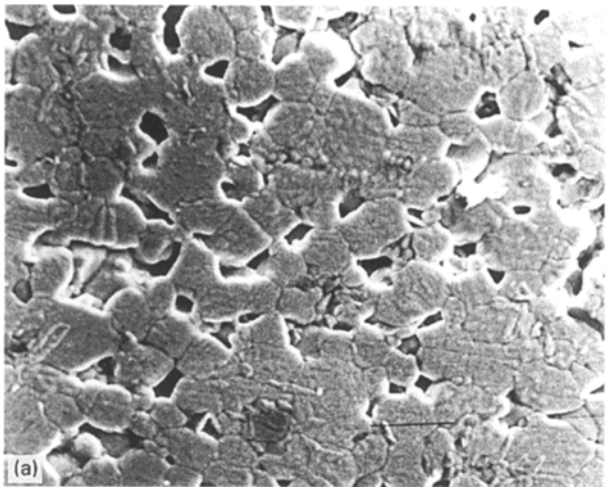

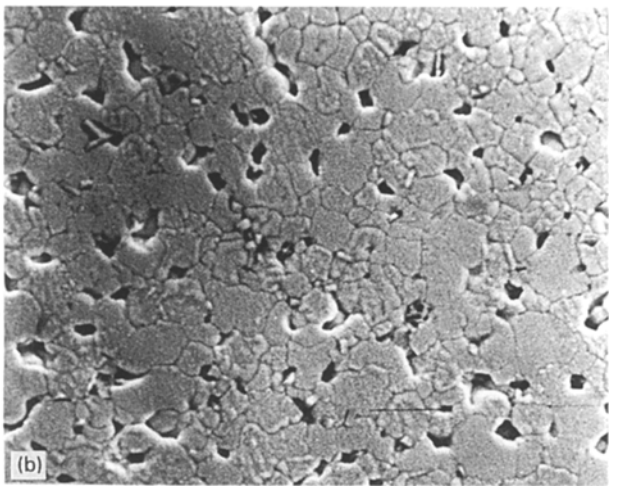

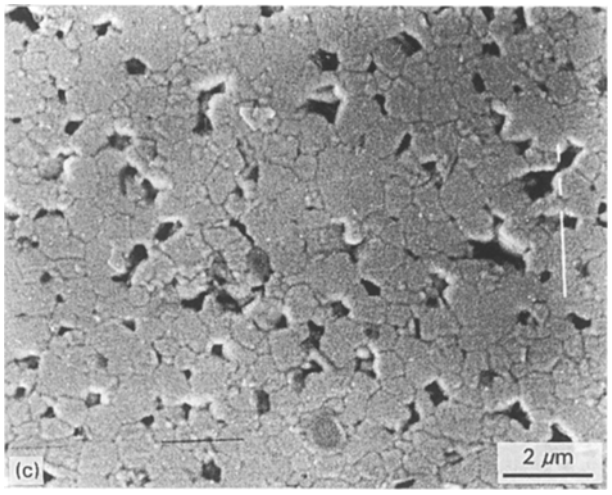

Figure 7 Micrographs of (a) PTC-24 ceramics, (b) PTC-30 ceramics and (c) PTC-35 ceramics.

has been shown for titanate perovskites that in some cases, Ti^{4+} can also be replaced by Ca^{2+} creating oxygen vacancies [19].

Therefore, the excess and segregation of titanium, calcium, cobalt, tungsten and manganese measured in these ceramics (PTC-24, PTC-30 and PTC-35) are indicative of formation of defects in crystal structures probably due to vacancies of lead and oxygen. However, it is not possible to calculate quantity of vacancies with the experimental techniques used in this work.

Piezoelectric behaviour of PTC-24, PTC-30 and PTC-35 ceramics is depicted in Fig. 8. It is observed that the field, E_p, necessary to get saturation in poling,

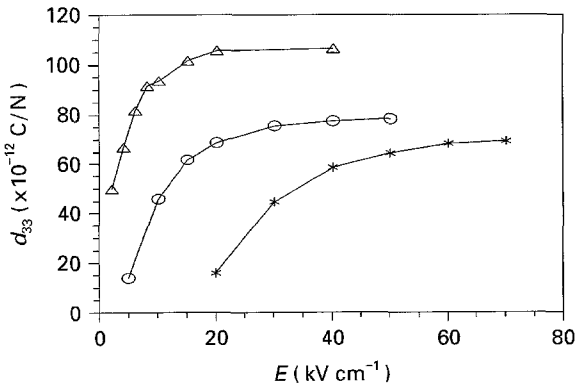

Figure 8 d_{33} piezoelectric coefficients versus electric poling field for the PTC-24 (*), PTC-30 (○) and PTC-35 (△) ceramics.

decreases with the increase in calcium content [20]. Therefore, lower electric fields are applied in PTC-35 samples than in PTC-30 samples than in PTC-24 samples, to study the intensity response of these materials versus frequency of a sinusoidal thermal wave (Fig. 9a–c).

Fig. 9a shows total electric currents stimulated by a sinusoidal thermic wave in PTC-24 ceramics and measured in face (−) and face (+) as a function of frequency and at different electric poling fields. The intensity response produced in face (−) is about 60% of the response of face (+). This intensity ratio stays constant over the whole range of the poling field studied. The behaviour of PTC-35 materials is similar to PTC-24 materials at low electric poling fields (Fig. 9c). However, an increase of intensity response of face (−) is observed in the former material, when the electric field increases, leading to higher currents measured in face (−) than in face (+) at high electric fields.

An intermediate behaviour is observed in PTC-30 samples. For fields $\leqslant 5$kV cm^{-1} intensities measured in face (+) always are higher than intensities measured in face (−). However, the intensity ratio of both faces decreases with the increase of electric field and they have very close responses when $E_p \geqslant 15$ V cm^{-1} (Fig. 9b).

Non-pyroelectric currents are calculated for each composition and as a function of thermic wave frequency, from values of total currents and taking account of the formula $i_{so} = i_{to} \sin \theta$. Fig. 10a and b show non-pyroelectric currents in PTC-24 and PTC-35 samples for different electric poling fields and frequencies. The behaviour of these currents is similar to those ones observed for total currents. Non-pyroelectric currents of face (+) are higher than non-pyroelectric currents of face (−), at low electric fields. When the field increases, non-pyroelectric response of these materials is affected by the quantity of calcium. Thus, non-pyroelectric currents measured in face (+) are higher than non-pyroelectric currents of face (−) for PTC-24 samples. The ratio between these currents stays constant with electric field. However, for PTC-35 samples it is observed that an increase of

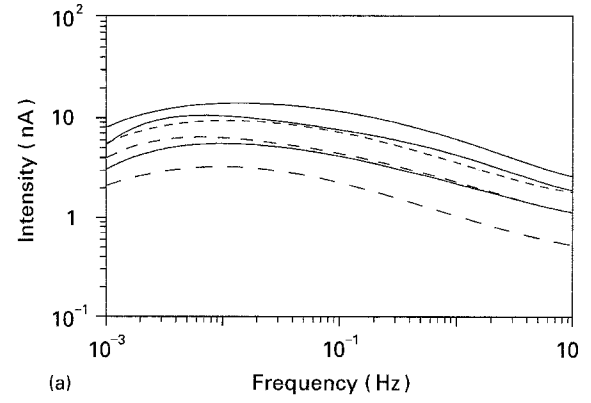

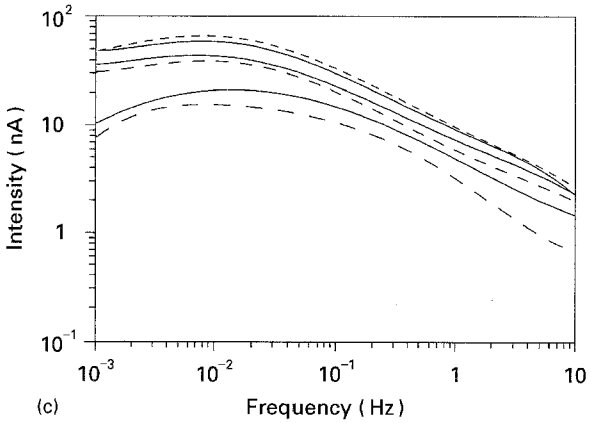

Figure 9 Total currents versus frequency of a sinusoidal thermal wave at different electric poling fields and in both faces of the ceramic for (a) PTC-24, (20, 40 and 70 kV cm^{-1}), (b) PTC-30, (5, 15 and 30 kV cm^{-1}) and (c) PTC-35, (2, 4 and 8 kV cm^{-1}). —— face (+); ---- face (—).

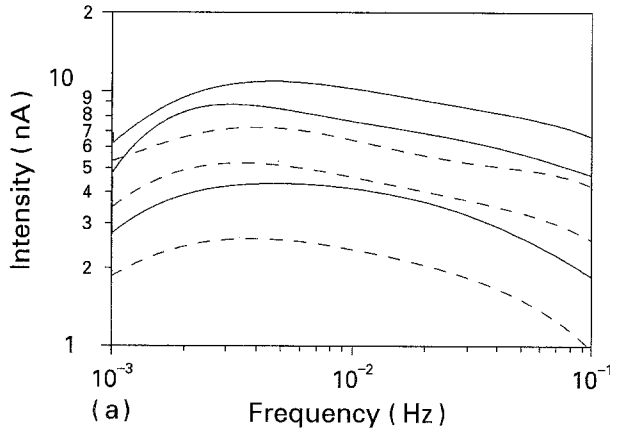

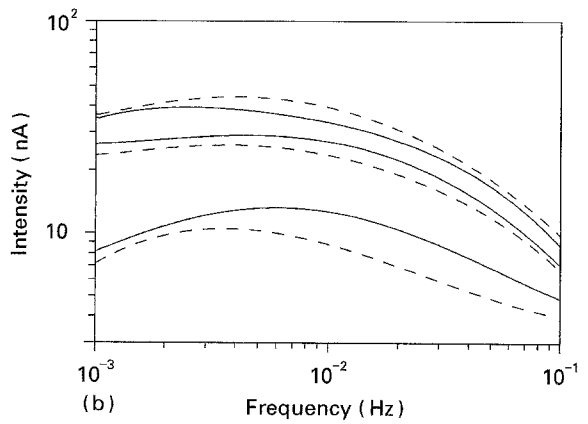

Figure 10 Non-pyroelectric currents versus frequency in (a) PTC 24, (20, 40 and 70 kV cm^{-1}) and (b) PTC-35 (2, 4 and 8 kV cm^{-1}) materials. —— face (+); ---- face (—).

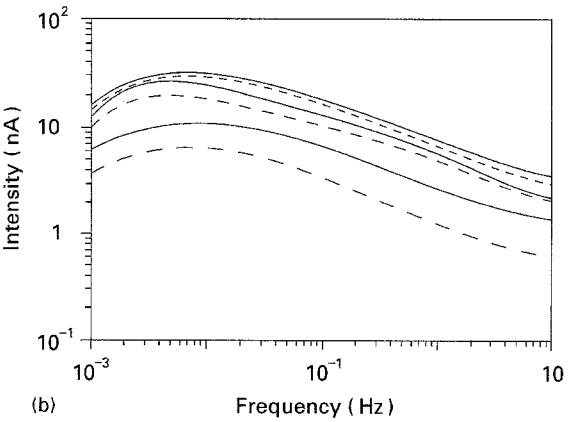

non-pyroelectric currents of face (−) with the field, leading to a higher response in face (−) than in face (+) for high electric poling fields.

From these studies, it can be deduced that these PTC ceramics show non-uniform spatial distributions of charge when excited by a thermal wave and under an applied electric field. In general, a higher density of charge is measured in face (+) than in face (−). However, a tendency to equilibrate charge distribution in both electrodes is observed with the increase of poling field and calcium content. These results can be summarized as follows

$$\text{PTC-24 } I_{\text{face}(+)} > I_{\text{face}(-)}$$

$$\text{PTC-30 } I_{\text{face}(+)} > I_{\text{face}(-)}\ E_p\uparrow\ I_{\text{face}(+)} \geqslant I_{\text{face}(-)}$$

$$\text{PTC-35 } I_{\text{face}(+)} \approx I_{\text{face}(-)}\ E_p\uparrow\ I_{\text{face}(+)} \leqslant I_{\text{face}(-)}$$

This behaviour indicates the existence of two types of charge carriers in the material. A high density of charge close to face (+), or positive electrode, is indicative of mobility of negative carriers. The contrary fact corresponds to displacement of positive carriers.

Considering the EDXA results previously shown, it can be deduced that these negative and positive carriers correspond to lead and oxygen vacancies. These ionic defects are created not only by loss of PbO during sintering of PTC ceramics, but also by substitution of some Ti^{4+} by Ca^{2+} [19]. Thus, the increase of calcium content in the material seems to increase oxygen vacancies. Besides, it is observed that a higher mobility of lead vacancies than oxygen vacancies occurs because higher electric fields have to be applied to move positive carriers to the negative electrode of face (−) (see Fig. 9a–c) [21].

4. Conclusions

Volatilization of PbO during sintering of modified lead titanate ceramics leads to compositional deviations from nominal chemical compositions of these materials.

Defect of lead and excesses of titanium, calcium, tungsten, cobalt and manganese are measured by EDX analysis on ceramic microstructures. The imbalance in chemical compositions causes lead and oxygen vacancies in perovskite structure. These vacancies behave as negative and positive charge carriers

that are excited by a thermal wave and under an electric field produce an intensity response in the material. In these conditions, it is observed that a non-uniform distribution of ionic defects is related to the content of calcium in the ceramics and with the poling field applied.

5. References

1. B. JIMÉNEZ, J. MENDIOLA, C. ALEMANY, L.DEL OLMO, L. PARDO, E. MAURER, M. L. CALZADA, J. DE FRUTOS, A. M. GOZÁLEZ and M. C. FANDIÑO, *Ferroelectrics* **87** (1988) 97.
2. Y. YAMASHITA, K. YOKOYAMA, H. HONDA and T. TAKAHASHI, *Jap. J. Appl. Phys.* **20** (1981) 183.
3. M. L. CALZADA and J. DE FRUTOS, *Mat. Res. Bull.* **28** (1993) 967.
4. K. WOJCIK, *Ferroelectrics* **82** (1988) 25.
5. T. YAMAMOTO, *Ceram. Bull* **71(6)** (1992) 978.
6. S. SHIRASAKI, K. TAKAHASHI and K. MANABE, *Bull. Chem. Soc. Jpn.* **44** (1971) 3189.
7. L. DEL OLMO, C. FANDIÑO, J. I. PINA, C. ALEMANY, J. MENDIOLA, L. PARDO, B. JIMÉNEZ and E. MAURER, Spanish Patent of Invention 555469, May 1986.
8. J. DE FRUTOS and B. JIMÉNEZ, *Ferroelectrics* **109** (1990) 101.
9. S. B. LANG and Q. R. YIN, *ibid.* **74** (1987) 357.
10. L. E. GARN and E. SHARP, *J. Appl. Phys.* **53** (1982) 8974.
11. D. R. DE VILLIERS and H. K. SCHMID, *J. Mater. Sci.* **25** (1990) 3215.
12. M. L. CALZADA and J. DE FRUTOS, *J. Mater. Sci. Mater. Elec.* **4** (1993) 83.
13. R. B. ATKIN and R. M. FULRATH, *J. Amer. Ceram. Soc.* **54** (1971) 265.
14. S. SHIRASAKI, *Solid State Comm.* **9** (1971) 1217.
15. S. SHIRASAKI, K. TAKAHASHI, H. YAMAMURA, K. KAKEGAWA and J. MORI, *J. Solid State Chem.* **12** (1975) 84.
16. G. H. DAI, P. W. LU, X. Y. HUANG, Q. S. LIU and W. R. XUE, *J. Mater. Sci. Mater. Elec.* **2** (1991) 164.
17. R. L. HOLMAN and R. M. FULRATH, *J. Appl. Phys.* **44** (1973) 5227.
18. K. H. HÄRDTL, *J. Amer. Ceram. Soc.* **64** (1981) 283.
19. Y. H. HAN, J. B. APPLEBY and D. M. SMYTH, *ibid.* **70(2)** (1987) 96.
20. J. MENDIOLA, L. PARDO, F. CARMONA and A. M. GONZÁLEZ, *Ferroelectrics* **109** (1990) 125.
21. J. CHEN, M. P. HARMER and D. M. SMYTH, Proceedings of the eighth IEEE, edited by M. Liu, A. Safari, A. Kingon and G. Haertling. Greenville SC, USA, September 1992, p. 111.

Received 23 February
and accepted 14 November 1994